

DMD 9928

FORMATION OF N-ALKYLPROTOPORPHYRIN IX FROM METABOLISM OF DIALLYL SULFONE IN LUNG AND LIVER

GORDON P. BLACK, KATHY S. COLLINS, DYLAN P. BLACQUIERE AND POH-GEK

FORKERT

Department of Anatomy and Cell Biology (G.P.B., K.S.C., D.P.B., P.-G.F.),

Queen's University, Kingston, Ontario, Canada

Running Title: N-Alkylprotoporphrin IX Formation from Diallyl Sulfone

Address correspondence to: Dr. Poh-Gek Forkert
Department of Anatomy and Cell Biology
Queen's University
Kingston, Ontario
Canada K7L 3N6
Phone: (613) 533-2854
Fax: (613) 533-2566
E-mail: forkertp@post.queensu.ca

Text pages:	19
Tables:	1
Figures:	9
References:	20
Abstract:	249
Introduction:	518
Results and Discussion:	1055
Section Assignment:	Short Communication

¹Abbreviations used are: AIA, allylisopropylacetamide; *N*-alkylPP, *N*-alkylprotoporphyrin IX; *N*-ethylPP, *N*-ethylprotoporphyrin IX; DAS, diallyl sulfide; DASO, diallyl sulfoxide; DASO₂, diallyl sulfone; DASO₃, 1,2-epoxypropyl-3,3'-sulfonyl-1'-propene.

ABSTRACT:

Diallyl sulfone (DASO₂) is a garlic derivative formed during cooking or after ingestion. Bioactivation of DASO₂ in murine lung and liver results in formation of an epoxide that inactivates CYP2E1 and significantly decreases cytochrome P450 and heme levels. In this study, we tested the hypothesis that DASO₂ metabolism leads to production of the heme adduct, *N*-alkylprotoporphyrin IX (*N*-alkylPP). Formation of *N*-alkylPP in vivo and in vitro was determined by spectrophotometric and fluorometric methods, respectively. In in vivo studies, *N*-alkylPP was generated in the livers of male and female mice treated with DASO₂, but was not detectable in the lungs of DASO₂-treated mice. In in vitro studies, rates of formation of *N*-alkylPP in liver and lung microsomes incubated with DASO₂ and NADPH were dependent on time and protein concentrations, and were negligible in control incubations performed in the absence of NADPH or DASO₂ or with boiled microsomes. The rates of *N*-alkylPP formation generated in murine liver were higher than in either murine lung or human liver. Kinetic analysis revealed that murine liver microsomes metabolized DASO₂ to *N*-alkylPP with higher affinity and catalytic efficiency than did murine lung or human liver microsomes. Recombinant rat CYP2E1 also metabolized DASO₂ to *N*-alkylPP; however, rates of formation of the heme adduct was minimal in incubations of recombinant human CYP2E1 with DASO₂. These findings demonstrated that the *N*-alkylPP adduct was produced via metabolism of DASO₂ in murine liver and lung microsomes, in human liver microsomes, in recombinant CYP2E1 and in vivo in murine liver.

In 1892, Semmler, a German chemist, applied steam distillation to cloves of garlic (*Allium sativum*) and produced a strong-smelling oil that on further purification produced diallyl sulfides (Block, 1985). The odoriferous constituent of garlic is allicin, which is formed by enzymatic conversion of *S*-allylcysteine sulfoxide (alliin) by alliinase to allicin. Allicin is an unstable component that can be further transformed to other garlic compounds including diallyl sulfide (DAS¹). In addition to being a component of garlic oil, DAS can be produced during cooking or after ingestion of garlic (Hayes et al., 1987). It has been estimated that 1 g of garlic yields approximately 30 to 100 µg of DAS (Sparnins et al., 1988).

Previous studies have identified both diallyl sulfoxide (DASO) and diallyl sulfone (DASO₂) in extracts of liver, blood and urine from rats treated with DAS, suggesting that DASO and DASO₂ are derived from DAS (Brady et al., 1991a). Studies with rat liver microsomes indicated that DAS undergoes sequential metabolism to DASO and DASO₂. Further studies confirmed that CYP2E1 catalyzes oxidation of the sulfur atom of DAS to yield DASO and subsequently DASO₂ (Jin and Baillie, 1997). Although these garlic derivatives are all competitive inhibitors of CYP2E1, the inhibitory effect of DASO₂ on CYP2E1 is more pronounced and is manifested more rapidly than by either DAS or DASO (Brady et al., 1991b). The efficacy of DASO₂ as a CYP2E1 inhibitor has been ascribed to mechanism-based inactivation, and it is the metabolic event involving DASO₂ that leads to CYP2E1 inactivation which mediates the chemoprotective effects of DAS (Jin and Baillie, 1997).

Previous studies have investigated the mechanisms responsible for the inactivation of CYP2E1 and the protective effective of DASO₂ against lung cytotoxicity induced by 1,1-dichloroethylene (Premdas et al., 2000; Forkert et al., 2000; Forkert et al., 1996). The results showed that DASO₂ undergoes P450-dependent oxidation at one of its terminal double bonds to

DMD 9928

form diallyl sulfone monoepoxide (1,2-epoxypropyl-3,3'-sulfonyl-1'-propene; DASO₃) (Fig. 1), a reactive metabolite believed to be responsible for CYP2E1 inactivation. Levels of immunodetectable CYP2E1, total cytochrome P450 and heme were all reduced (Premdas et al., 2000). Incubation of murine liver microsomes with DASO₂ (1.0 mM) decreased total cytochrome P450 and heme levels by about 30% and 70%, respectively. Immunodetectable CYP2E1 was reduced, and correlated with a 70% decrease in *p*-nitrophenol hydroxylation 2 h after treatment of mice with DASO₂ (100 mg/kg, p.o.). These findings suggested the possibility that bioactivation of DASO₂ produces the reactive metabolite, DASO₃, that alkylates the heme moiety at one of the four pyrrole nitrogens within the active site of P450, yielding the heme adduct *N*-alkylprotoporphyrin IX (*N*-alkylPP; Fig. 2) (for review see Ortiz de Montellano and Correia, 1983, 1995). Here, we have undertaken studies to test the hypothesis that metabolism of DASO₂ leads to the formation of *N*-alkylPP, an event that is likely associated with loss of heme and inactivation of cytochrome P450 reported previously (Premdas et al., 2000). Our results confirmed that the *N*-alkylPP adduct is produced from oxidative metabolism of DASO₂ in murine liver and lung microsomes, in human liver microsomes, in recombinant rat CYP2E1 and in vivo in murine liver.

Materials and Methods

Materials. Chemicals and reagents were obtained from suppliers as follows: potassium phosphate, NADPH, dichloromethane (HPLC grade) sodium sulfate (anhydrous), zinc acetate and iodoethane (Sigma-Aldrich Canada Ltd., Oakville, ON, Canada); sulphuric acid (E. Merck, Stockholm, Sweden); protoporphyrin IX dimethyl ester (Frontier Scientific Porphyrin Products, Logan, Utah); Silica Gel G thin layer chromatography plates (1000 and 2000 µM) (Analtech,

Newark, DE.). Diallyl sulfone was synthesized by Colour Your Enzyme (Bath, ON, Canada). Human liver microsomes and recombinant rat and human CYP2E1 were obtained from BD Biosciences Discovery Labware (Bedford, MA). Allylisopropylacetamide (AIA) was a donation from Dr. Gerald S. Marks (Department of Pharmacology and Toxicology, Queen's University).

Animal Treatment. Male and female CD-1 mice, weighing 22 to 30 g, were obtained from Charles River Canada (St. Constant, QC, Canada). The mice were maintained on a 12 h light/dark cycle and were given free access to water and food (Mouse diet 5015; PMI Nutrition International Inc., Brentwood, MO). For the in vivo experiments, male and female mice were treated with 100 mg/kg DASO₂ in water (p.o.); control mice were treated with water. After 2 h, the mice were anaesthetized with sodium pentobarbital (120 mg/kg, i.p.), and were perfused with ice cold potassium chloride (1.15%) via the left ventricle. Once blood was flushed from the tissues, the lungs and livers were frozen in liquid nitrogen and stored at – 80°C. Human lung tissue (10-50 g) was obtained from Kingston General Hospital, (Kingston, Ontario) from consenting patients undergoing surgical lobectomies. The protocol for the studies in human lung was approved by Queen's University Human Ethics Committee. Tissues distant from the primary lesions were surgically excised, placed on ice and transferred to a biohazard facility.

Isolation and Purification of *N*-AlkylIPP. Preliminary studies were performed with AIA which has been shown to produce the *N*-alkylIPP adduct (Wong and Marks, 1999; Lavigne et al., 2002). Formation of *N*-alkylIPP as a result of *N*-alkylation of the heme moiety is believed to be one of the mechanisms involved in P450 inactivation (Halpert et al., 1994). It is recognized that the *N*-alkyl constituent of the heme adduct in this study has not been identified. However, the similar spectral characteristics of the *N*-alkylIPP adduct formed from AIA and those identified herein supported the assumption that the adduct formed from DASO₂ likely represents the *N*-

alkylPP adduct. For the *in vivo* studies, livers from 3 mice and lungs from 10 mice were pooled for each sample. Tissues were homogenized in ice-cold H₂SO₄ in methanol (5%, v/v; 10-15 ml/g tissue). The homogenates were stored in the dark at 4°C for 24 h, after which purification and isolation of *N*-alkylPP was performed according to a method described previously (Wong *et al.*, 1999). Briefly, the *N*-alkylPP dimethyl ester was isolated from the homogenates, reacted with zinc acetate (25 µmol) in methanol to form the Zn-*N*-alkylPP dimethyl ester and dried. The residue was dissolved in 2 ml of dichloromethane, applied to a gel G thin layer chromatography silica plate (2000 µm) and developed in dichloromethane:methanol (260:39, v/v) for 60 min. The single green band ($R_f = 0.68-0.74$) (Wong and Marks, 1999) that exhibited red fluorescence (corresponding to reacted dimethyl esters) under long-wave ultraviolet light was scraped off the plate, extracted with acetone and evaporated to dryness. The residue was then dissolved in 2 ml of methanol containing zinc acetate (25 µmol) and dried using a rotary evaporator. This final residue was dissolved in 2 ml of dichloromethane and the absorption spectrum of the sample was determined by scanning from 400 to 800 nm, using a Beckman DU 640B spectrophotometer. The concentration of Zn-*N*-alkylprotoporphyrin IX was estimated using the molar extinction coefficient ($\epsilon > 128,000 \text{ m}^{-1}\text{cm}^{-1}$ at 432 nm) for the Zn-*N*-ethylPP dimethyl ester (Ortiz de Montellano *et al.*, 1981).

Synthesis of Zn-*N*-EthylPP Dimethyl Ester. The adduct *N*-ethylprotoporphyrin IX (*N*-ethylPP) has been used in previous studies as an analog for other alkylated heme adducts (Lavigne *et al.*, 2002). The method of De Matteis *et al.* (1980) was used to synthesize *N*-ethylPP. Protoporphyrin-IX dimethyl ester (3.2 mg) was reacted with iodoethane (2 ml) for 18 h at 105°C in a sealed 5-ml test tube. The residue was purified by thin-layer chromatography using a silica plate (2000 µm) as described previously (Kimmett and Marks, 1992). The reacted dimethyl ester

was extracted with acetone, dried and resuspended in methanol containing zinc acetate (25 μ mol). The residue was subjected to thin-layer chromatography (1000 μ m) and the concentration of the Zn-*N*-ethylPP dimethyl ester determined by UV-visible spectrophotometry as described above. The emission spectra of known amounts of *N*-ethylPP dimethyl ester were determined on a fluorescence plate reader. The solution (200 μ l) was added to each well of a white 96-well microtitre plate and read on a fluorescence plate reader (Spectra MAX Gemini XS fluorescent plate reader/Softmax® PRO software), using an excitation wavelength of 432 nm (Soret peak) and an emission scan from 600 to 800 nm. The relative fluorescence units at 630 nm were used to determine the points of a standard concentration curve. There was a linear relationship between the amounts of *N*-ethylPP dimethyl ester and relative fluorescence units ($R^2 = 0.9841$) (Fig. 3). The lower limit of detection is 2.5 pmoles.

Preparation of Microsomes. Microsomes were isolated from male mice according to procedures used in our previous studies (Forkert, 1995). Livers from 3 male mice and lungs from 50 male mice were pooled for each microsomal sample. Human lung tissues were not pooled but were retained as individual samples. Human lung microsomes were prepared using procedures described previously (Forkert et al., 2001). Protein concentrations were determined using the method of Bradford (1976).

Microsomal Incubations. In murine microsomal incubations, reaction mixtures contained microsomal protein in 0.1 M phosphate buffer, pH 7.4, NADPH (2.0 mM) and DASO₂ (0 – 5.0 mM) in a total volume of 1 ml. Protein concentrations used for murine and human liver microsomal incubations were 0.5 to 5 mg, and for murine and human lung microsomal incubations were 1 to 5 mg. Incubations with recombinant rat and human CYP2E1 were carried out with 50 to 200 pmoles of enzyme, NADPH (2.0 mM) and DASO₂ (0 – 5.0 mM). Incubations

for time-course experiments were carried out between 0 to 40 min. Incubations for concentration-response studies were performed with 1 to 4.0 mM of DASO₂. All incubations were performed at 37°C. Controls included incubations performed in the absence of NADPH, DASO₂ or microsomes as well as incubations using boiled microsomes. After the incubations, *N*-alkylPP was isolated from the microsomes using the method described previously (Lavigne et al., 2002). The *N*-alkylPP was extracted into dichloromethane, the organic extract washed with sodium bicarbonate (5%, v/v) and water, reacted with zinc acetate (12 µmol) in methanol (1 ml), dried and dissolved in methanol. For lung and liver samples, 200 µl of the suspension were added to each well of a white 96-well microtitre plate, and read on a fluorescence plate reader (Spectra MAX Gemini XS fluorescent plate reader/Softmax® PRO software) using an excitation wavelength of 432 nm (Soret peak) and an emission scan from 600 to 800 nm. The amounts of *N*-alkylPP present in the sample were determined by relating fluorescence values at 630 nm to the *N*-ethylPP dimethyl ester standard curve.

Statistical Analysis. Data in the in vivo studies were expressed as mean ± S.D. and were analyzed using the Student's *t* test. The level of significance was set at $p < 0.05$. Michaelis-Menten kinetic analysis was performed by using GraphPad Prism version 4 (GraphPad Software Inc., San Diego, CA).

Results and Discussions

Previous studies indicated that metabolism of DASO and DASO₂ favors oxidation at the terminal double bonds, yielding epoxides that conjugated with glutathione (Jin and Baillie, 1997). More recent studies corroborated these findings and showed that an epoxide (DASO₃), was formed in murine lung and liver microsomal incubations containing DASO₂ and NADPH, and was not formed in the absence of NADPH (Forkert et al., 2000; Premdas et al., 2000). The formation of DASO₃ coincided with loss of immunodetectable CYP2E1 protein and associated *p*-nitrophenol hydroxylation; these findings are in agreement with studies in rat liver suggesting that DASO₂ is metabolized by CYP2E1 (Brady et al., 1991b). The significant loss of heme associated with DASO₂ led us to undertake studies to test the hypothesis that the *N*-alkylPP adduct is generated from its metabolism.

Studies were carried out in mice treated with DASO₂ to determine if the *N*-alkylPP adduct was formed in vivo. The identity of the *N*-alkylPP adduct was confirmed by characteristics of the absorption spectrum of the Zn-*N*-alkylprotoporphyrin IX as determined by UV-visible spectrophotometry; a major peak was observed at 432 nm and minor peaks at 547, 591 and 634 nm (Fig. 4A). The *N*-alkylPP adduct was detected in the livers of both male and female mice, with levels that were significantly higher in males than in females (Fig. 4B). The heme adduct was not detectable in the lungs of DASO₂-treated mice. These results confirmed that the *N*-alkylPP adduct was formed in vivo from DASO₂ in the liver but not in the lung. These findings are consistent with the considerably higher levels of cytochrome P450 found in the liver versus the lung, suggesting that the rates of adduct formation in the lung were too low to be detectable.

Identification of *N*-alkylPP in microsomal incubations was performed using a 96-well microtitre plate and a fluorescence plate reader. This strategy was adopted because lung

microsomes from mice were of low yield and the plate reader required only 200 μ l of sample vs. 2 ml in the cuvette for fluorometry as described in previous studies (Lavigne et al., 2002). Representative spectra obtained by fluorometry in liver and lung microsomal incubations are illustrated in Fig. 5. At an excitation wavelength of 432 nm, characteristic peaks were observed at 630 and 700 nm. The magnitudes of the peaks were greater in the liver (Fig. 5A) than in the lung (Fig. 5B) microsomal incubations. These peaks were not observed in microsomal incubations performed in the absence of NADPH (Fig. 5C) or DASO₂ (Fig. 5D), nor were they found in incubations performed with boiled microsomes (data not shown).

In murine and human liver microsomal incubations, the rates of formation of *N*-alkylPP from DASO₂ were both time-dependent and were incremental from 0 to 30 min, with declines at 40 min (Fig. 6A and 7A). The rates of adduct formation by murine liver microsomes were incremental with protein concentrations ranging from 0.5 to 2.0 mg, with saturation rates at 2 to 3 mg of protein. In incubations of human liver microsomes, the rates of *N*-alkylPP formation increased with protein concentrations of 0 to 3 mg, with saturation rates of adduct formation at 3 to 5 mg (Fig. 7B). In murine lung microsomal incubations, rates of formation of the heme adduct were linear from 0 to 20 min and decreased thereafter (Fig. 8A). Rates of adduct formation were also protein-dependent and were linear from 0 to 4.0 mg of protein, with saturation at 4 to 5 mg of protein concentration. Based on these data, DASO₂ concentration studies in murine liver were carried out with 1.5 mg of microsomal protein for 10 min, in human liver with 1.5 mg of microsomal protein for 8 min, and in murine lung with 2.0 mg of microsomal protein for 10 min. The results showed that the rates of *N*-alkylPP adduct formation were highly correlated with DASO₂ concentrations used in the incubations of microsomes from

murine liver ($R^2 = 0.9936$) (Fig. 6C), human liver ($R^2 = 0.9816$) (Fig. 7C), and murine lung ($R^2 = 0.9741$) (Fig. 8C).

The results of Michaelis-Menten kinetic analysis of the DASO₂ concentration-dependent studies are illustrated in Figs. 6C, 7C and 8C, and the kinetic constants obtained are given in Table 1. The apparent K_m for murine liver microsomes was 2.9-fold lower than that for murine lung microsomes, which was similar to the apparent K_m for human liver microsomes. The apparent V_{max} for murine liver microsomes was similar to the apparent V_{max} for lung microsomes, but was about 2-fold lower than in human liver microsomes. These data yielded apparent V_{max}/K_m ratios that were 1.3-fold higher for murine liver microsomes than for human liver microsomes. However, the V_{max}/K_m ratios for both murine and human liver microsomes were about 3- and 2-fold higher, respectively, than for murine lung microsomes. Formation of *N*-alkylPP was not detected in incubations of human lung microsomes. These results indicated that the catalytic affinities and efficiencies for metabolism of DASO₂ to *N*-alkylPP were higher in murine liver microsomes than in either murine lung or human liver microsomes. However, the values for the V_{max} and the V_{max}/K_m ratio found for the human liver microsomes suggested that formation of *N*-alkylPP may be a relevant event in DASO₂ metabolism in the human.

Previous studies have reported that CYP2E1 is inhibited by DASO₂ in lung and liver of mice (Forkert et al., 2000; Premdas et al., 2000). In order to determine the role of CYP2E1 in producing the *N*-alkylPP adduct, incubations of DASO₂ were carried out with recombinant rat and human CYP2E1 enzymes. The heme adduct was generated in incubations of recombinant rat CYP2E1 with DASO₂ in a time- and protein-concentration manner (data not shown). Kinetic analysis of data from concentration-dependent studies yielded an apparent K_m of 0.35 ± 0.11 mM and an apparent V_{max} of 7.3 ± 0.9 pmol/min/nmol CYP2E1 ($V_{max}/K_m = 20.86$). These results

supported the contention that the recombinant rat CYP2E1 enzyme has a high catalytic efficiency for formation of the *N*-alkylPP adduct, and is consistent with the inactivation of CYP2E1 found in previous studies (Premdas et al., 2000). Incubations of recombinant human CYP2E1 with DASO₂ produced minimal levels of *N*-alkylPP and were too low for kinetic analysis.

In summary, the results of these studies demonstrated that metabolism of DASO₂ leads to formation of the *N*-alkylPP adduct by murine liver and lung microsomes, by human liver microsomes, by recombinant rat CYP2E1 and in vivo in murine liver, and supported the contention that P450 inactivation by DASO₂ is associated with *N*-alkylation of the heme moiety.

Acknowledgments

We thank Dr. Gerald S. Marks for advice and assistance to this study.

References

- Block E (1985) The chemistry of garlic and onion. *Sci Am* **252**:114-119.
- Bradford MM (1976) A rapid and sensitive method for the quantitation of microgram quantities of protein utilizing the principle of protein-dye binding. *Anal Biochem* **72**:248-254.
- Brady JF, Wang M-H, Hong J-Y, Xiao F, Li Y, Yoo J-SH., Ning SM, Lee M-J, Fukuto, JM, Gapac JM, and Yang CS (1991a) Modulation of rat hepatic microsomal monooxygenase enzymes and cytotoxicity by diallyl sulfide. *Tox Appl Pharmacol* **108**:342-354.
- Brady JF, Li DC, Ishizaki H, Fukuto JM, Lin MC, Fadel A, Gapac JM, and Yang CS (1991b) Inhibition of cytochrome P-450 2E1 by diallyl sulfide and its metabolites. *Chem Res Toxicol* **4**:642-647.
- De Matteis F, Gibbs AH, Cantoni L, and Francis J (1980) Substrate-dependent irreversible inactivation of cytochrome P-450: conversion of its haem moiety into modified porphyrins. *Ciba Foundation Symposium* **76**:119-139.
- Forkert PG, Dowsley TF, Lee RP, Hong J-Y, and Ulreich JB (1996) Differential formation of 1,1-dichloroethylene-metabolites in the lungs of adult and weanling male and female mice: correlation with severities of bronchiolar cytotoxicity. *J Pharmacol Exp Ther* **279**:1484-1490.
- Forkert PG, Lee RP and Reid K (2001) Involvement of CYP2E1 and carboxylesterase enzymes in vinyl carbamate metabolism in human lung microsomes. *Drug Metab Dispos* **29**:258-263.
- Forkert PG, Lee RP, Dowsley TF, Hong J-F, and Ulreich JB (1996) Protection from 1,1-dichloroethylene-induced Clara cell injury by diallyl sulfone, a derivative of garlic. *J Pharmacol Exp Ther* **277**:1665-1671.

- Forkert PG, Premdas PD, and Bowers RJ (2000) Epoxide formation from diallyl sulfone is associated with CYP2E1 inactivation in murine and human lungs. *Am J Respir Cell Mol Biol* **23**:687-695.
- Halpert JR, Guengerich FP, Bend JR, and Correia MA (1994) Selective inhibitors of cytochromes P450. *Toxicol Appl Pharmacol* **125**:163-175.
- Hayes MA, Rushmore TH, and Goldberg MT (1987) Inhibition of hepatic carcinogenic responses to 1,2-dimethylhydrazine by diallyl sulfide, a component of garlic oil. *Carcinogenesis (Lond)* **8**:1155-1157.
- Jin L, and Baillie TA (1997) Metabolism of the chemoprotective agent diallyl sulfide to glutathione conjugates in rats. *Chem Res Toxicol* **10**:318-327.
- Kimett SM and Marks GS (1992) Thin-layer chromatographic separation of the ferrochelataase-inhibitory ring A and ring B regioisomers of *N*-ethylprotoporphyrin from a mixture of the four regioisomers. *J Pharmacol Toxicol Methods* **28**:113-117.
- Lavigne JA, Nakatsu K, and Marks GS (2002) Identification of human hepatic cytochrome P450 sources of *N*-alkylprotoporphyrin IX after interaction with porphyrinogenic xenobiotics, implications for detection of xenobiotic-induced porphyria in humans. *Drug Metab Dispos* **30**:788-794.
- Ortiz de Montellano PR, and Correia MA (1983) Suicidal destruction of cytochrome P-450 during oxidative drug metabolism. *Annu Rev Pharmacol Toxicol* **23**:481-503.
- Ortiz de Montellano PR, and Correia MA (1995) Inhibition of cytochrome P450 enzymes. In *Cytochrome P450: Structure, Mechanism and Biochemistry* (Ortiz de Montellano P. R. Ed.) pp.305-364. Plenum Press, New York.

DMD 9928

- Ortiz de Montellano PR, and Mico BA (1981) Destruction of cytochrome P-450 by allylisopropylacetamide is a suicidal process. *Arch Biochem Biophys* **206**:43-50.
- Premdas PD and Bowers RJ, and Forkert PG (2000) Inactivation of hepatic CYP2E1 by an epoxide of diallyl sulfone. *J Pharmacol Exp Ther* **293**:1112-1120.
- Sparnins VL, Barany G, and Wattenberg LW (1988) Effects of organosulfur compounds from garlic and onions on benzo[a]pyrene-induced neoplasia and glutathione *S*-transferase activity in the mouse. *Carcinogenesis* **9**:131-134.
- Wong GW, Kobus SM, KcNamee JP, and Marks GS (1998) Gender differences in *N*-alkylprotoporphyrin IX production in rats after the administration of porphyrinogenic xenobiotics. *Drug Metab Dis* **26**:739-744.
- Wong SGW and Marks GS (1999) Formation of *N*-alkylprotoporphyrin IX after interaction of porphyrinogenic xenobiotics with rat liver microsomes. *J Pharmacol* **42**:107-113.

DMD 9928

Footnotes

- a) This study was funded by Grant # 014061 from the National Cancer Institute of Canada.
- b) Address correspondence to: Dr. Poh-Gek Forkert, Department of Anatomy and Cell Biology, Queen's University, Kingston, ON, Canada K7L 3N6. Email:forkertp@post.queensu.ca

Figure Legends

Fig. 1. Scheme of metabolism of diallyl sulfone to diallyl sulfone monooxide (A).

Fig. 2. Structure of *N*-alkylprotoporphyrin IX (the alkyl group could be on any of the pyrrole rings).

Fig. 3. Regression analysis of concentrations of synthesized *N*-ethylprotoporphyrin IX and relative fluorescence units (RFU). The values were used as a standard curve for determination of *N*-alkylPP formation in incubations of microsomes and recombinant CYP2E1.

Fig. 4. Absorption spectrum (A) and formation (B) of the zinc complexed *N*-alkylPP dimethyl ester in liver homogenates from female and male mice treated with DASO₂. *, Significantly different from levels in female mice.

Fig. 5. Fluorescence spectra obtained from incubation of DASO₂ (2.0 mM) and NADPH (2.0 mM) with liver (A) and lung (B) microsomes. Controls comprised of incubations performed in the absence of DASO₂ (C) or NADPH (D).

Fig. 6. Time- (A) and protein-dependent (B) formation of the *N*-alkylPP adduct in incubations of murine liver microsomes with DASO₂ (2.0 mM) and NADPH (2.0 mM). Kinetic analysis of data from incubations of the microsomes with various DASO₂ concentrations and NADPH (C).

Fig. 7. Time- (A) and protein-dependent (B) formation of the *N*-alkylPP adduct in incubations of human liver microsomes with DASO₂ (2.0 mM) and NADPH (2.0 mM). Kinetic analysis of data from incubations of the microsomes with various DASO₂ concentrations and NADPH (C).

Fig. 8. Time- (A) and protein-dependent (B) formation of the *N*-alkylPP adduct in incubations of murine lung microsomes with DASO₂ (2.0 mM) and NADPH (2.0 mM). Kinetic analysis of incubations of the microsomes with various DASO₂ concentrations and NADPH (C).

DMD 9928

Fig. 9. Kinetic analysis of data from incubations of recombinant rat CYP2E1 (150 pmol) with DASO₂ (2.0 mM) and NADPH (2.0 mM).

TABLE 1

Kinetic analysis of DASO₂ metabolism to *N*-alkylPP in incubations of murine liver and lung microsomes and human liver microsomes. Reaction mixtures in a total volume of 1.0 ml of 0.1 M potassium phosphate buffer, pH 7.4, contained murine liver microsomes (1.5 mg protein), murine lung microsomes (2.0 mg protein), human liver microsomes (1.5 mg protein), human lung microsomes (5 mg protein), 2 mM NADPH and concentrations of DASO₂ ranging from 0 to 5.0 mM.

	K_m	V_{max}	V_{max}/K_m
Murine liver microsomes	0.85 ± 0.07 mM	1.43 ± 0.03 nmol/min/mg protein	1.68
Murine lung microsomes	2.48 ± 0.07 mM	1.33 ± 0.11 nmol/min/mg protein	0.54
Human liver microsomes	2.41 ± 0.31 mM	3.03 ± 0.19 nmol/min/mg protein	1.26
Human lung microsomes	N.D.		

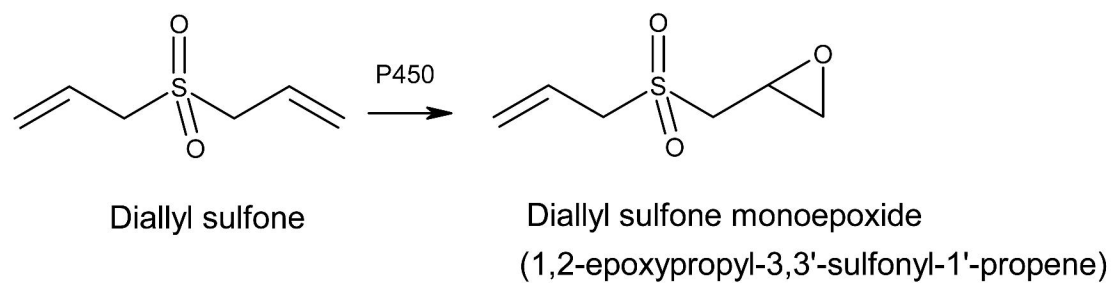


Figure 1

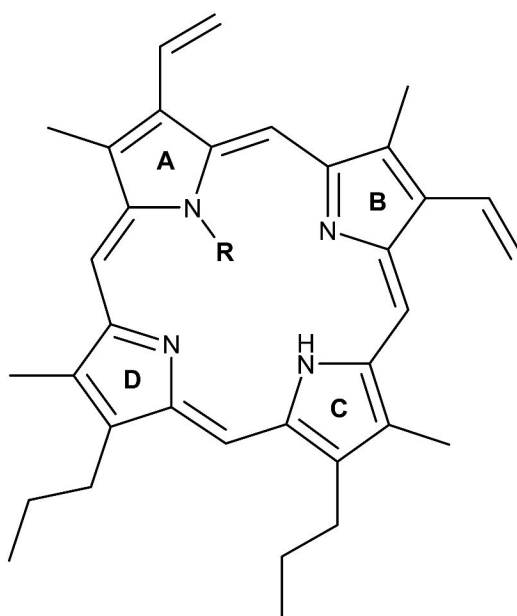


Figure 2

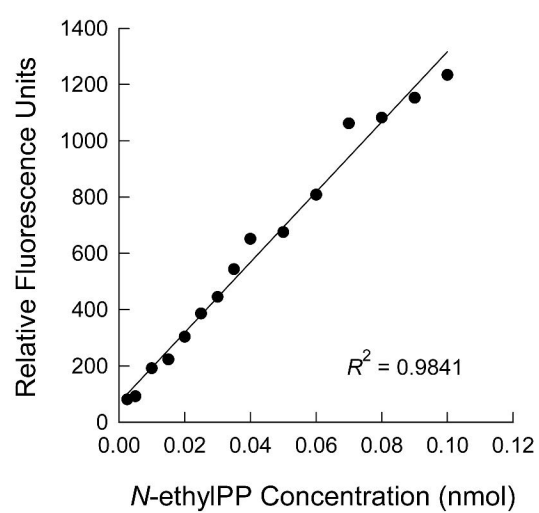


Figure 3

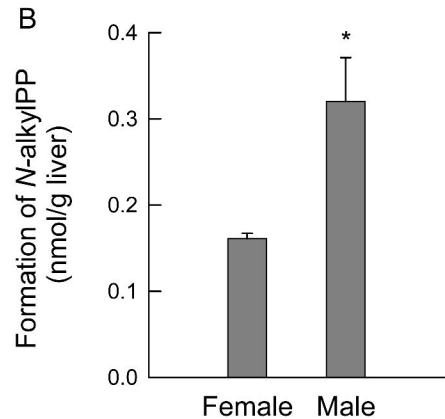
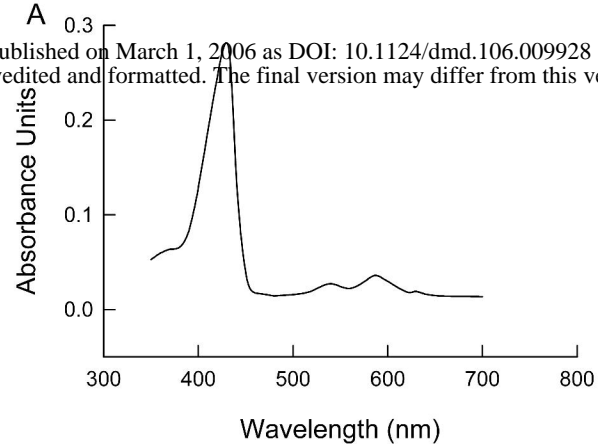


Figure 4

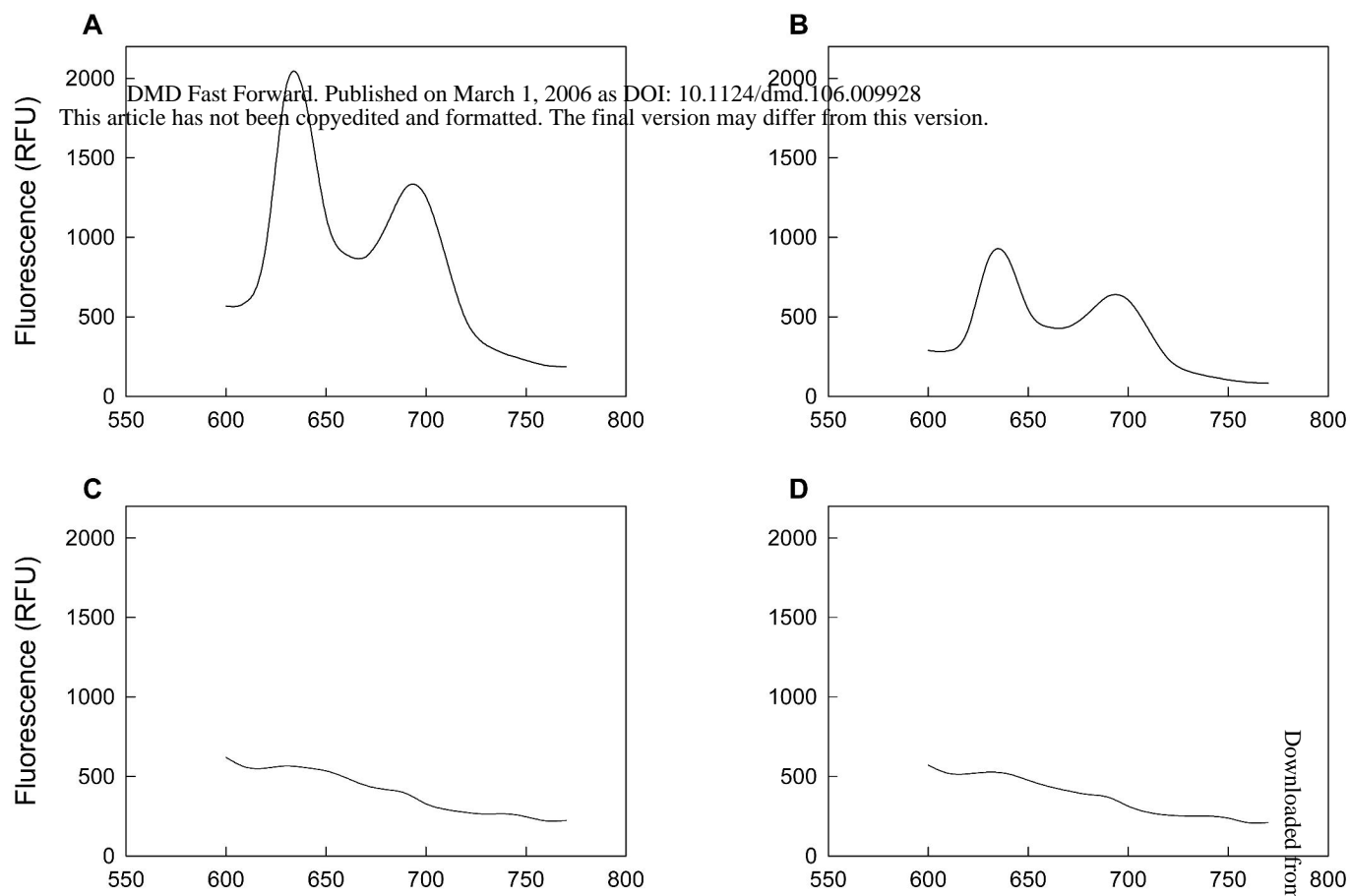


Figure 5

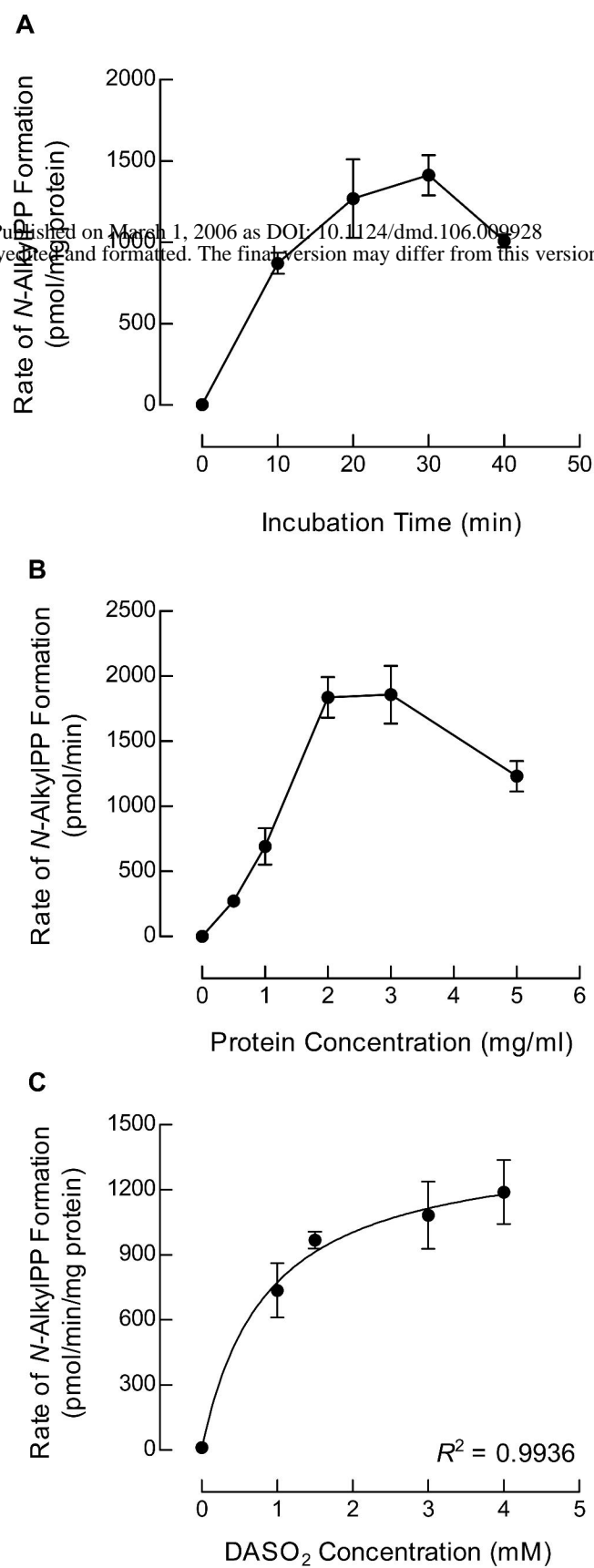


Figure 6

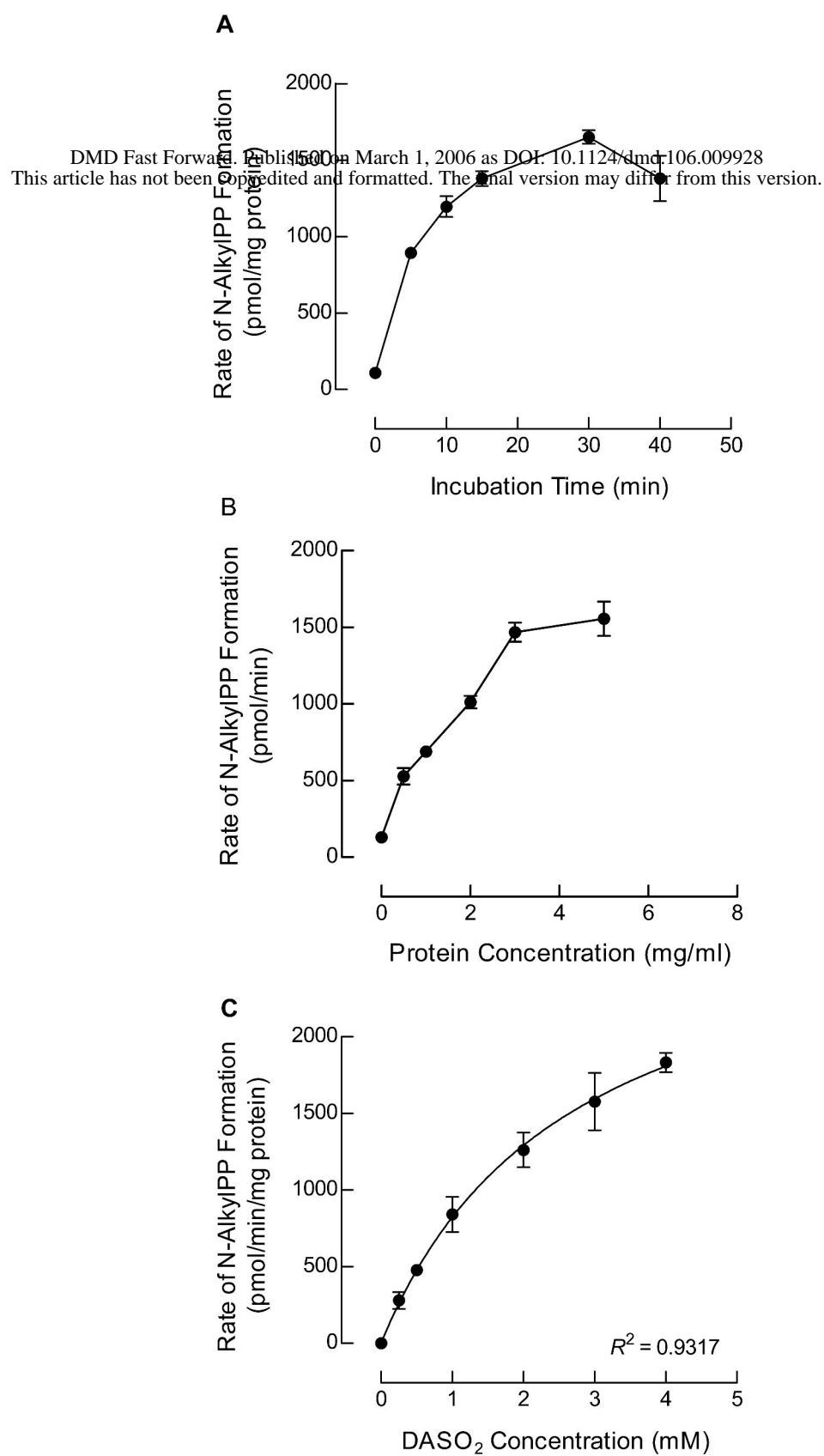


Figure 7

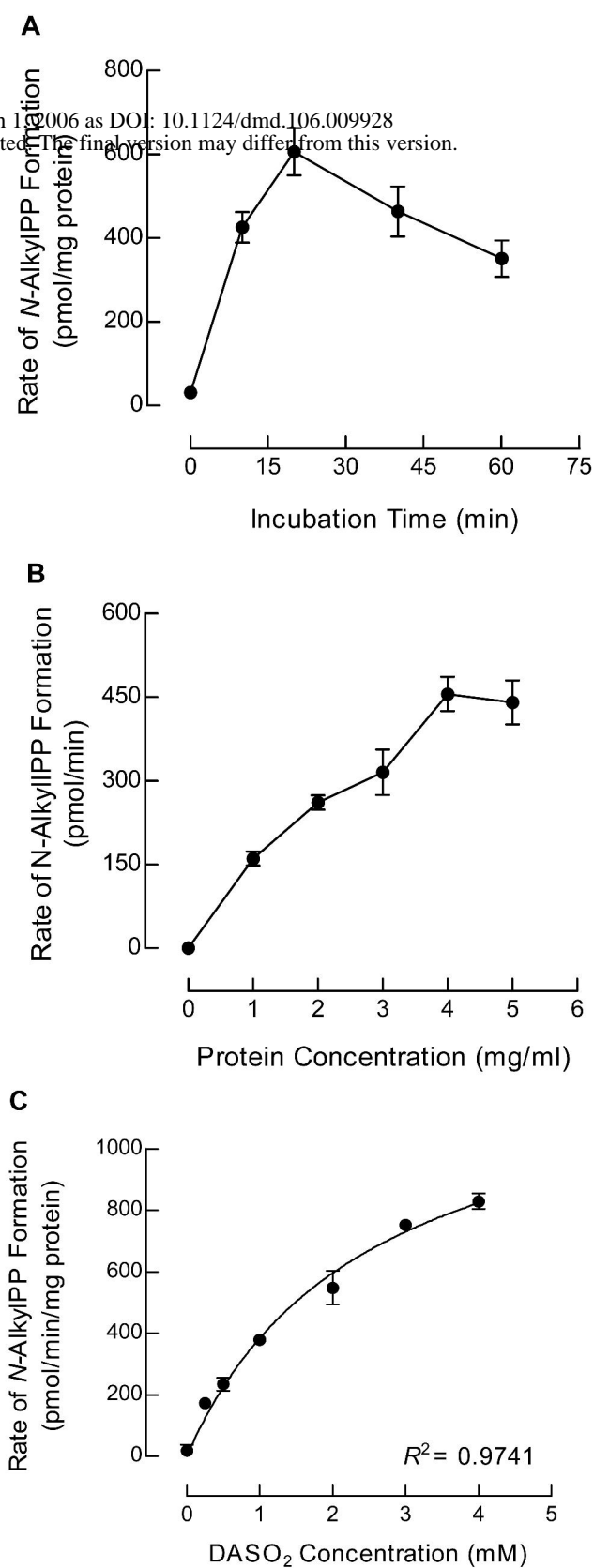


Figure 8

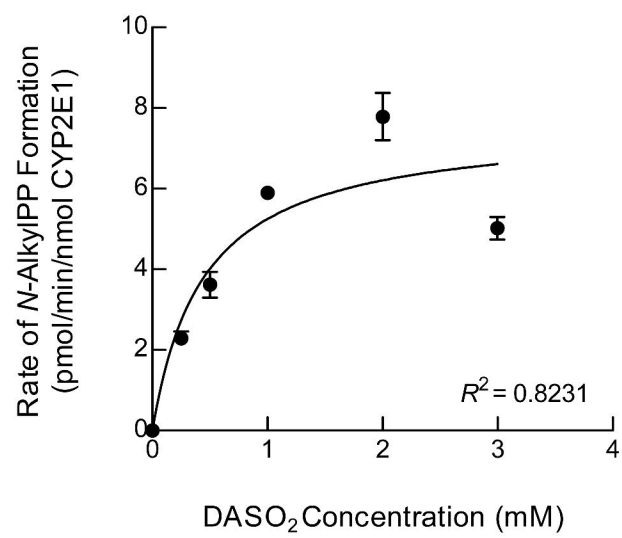


Figure 9